Supporting Information

Tris(Carbene)-Stabilization of Monomeric Magnesium Cations: A Neutral, Non-tethered Ligand Approach

Akachukwu D. Obi,† Jacob E. Walley,† Nathan C. Frey,‡ Yuen Onn Wong,† Diane A. Dickie,† Charles Edwin Webster,‡ Robert J. Gilliard, Jr.†**

† Department of Chemistry, University of Virginia, 409 McCormick Road, PO Box 400319, Charlottesville, Virginia 22904, United States

‡ Department of Chemistry, Mississippi State University, Box 9573, Mississippi State, Mississippi 39762, United States

*To whom correspondence should be addressed: rjg8s@virginia.edu, ewebster@chemistry.msstate.edu

Table of Contents

Crystal Structure of 3[BAr$^{F}_{4}$]

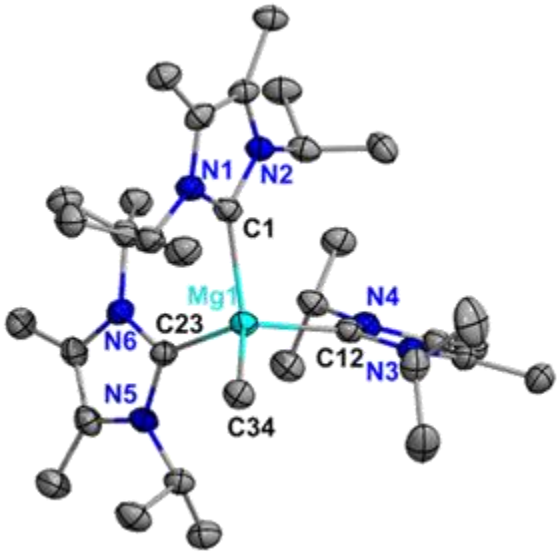

Figure S1: X-ray structure of **3[BAr$^{F}_{4}$]** (thermal ellipsoids shown at 30% probability; H atoms and BAr$^{F}_{4}$ anion are omitted for clarity). Selected bond distances (Å) and angles (º): Mg1–C1: 2.281(6); Mg1–C12: 2.276(6); Mg1–C23: 2.262(5); Mg1–C34: 2.154(5); C1–Mg1–C12: 108.85(19); C1–Mg1–C23: 111.4(2); C1–Mg1–C34: 109.8 (2); C12–Mg1–C23: 103.6(2); C12–Mg1–C34: 112.1(2); C23–Mg1–C34: 111.0(2).

Crystal Structure of 4[BAr$^{F}_{4}$]

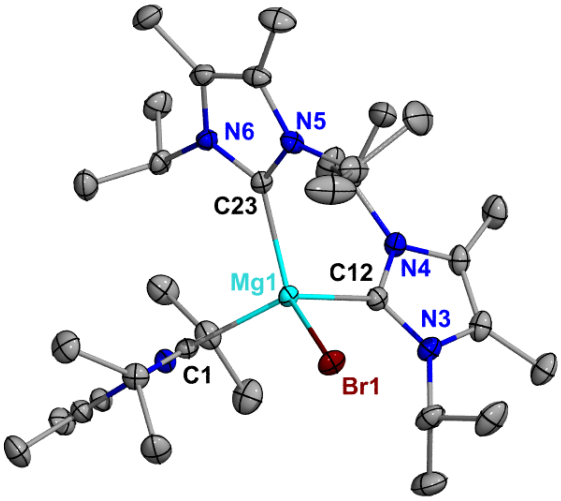

Figure S2: X-ray structure of **4[BAr$^{F}_{4}$]** (thermal ellipsoids shown at 50% probability; H atoms and BAr$^{F}_{4}$ anion are omitted for clarity). Selected bond distances (Å) and angles (º): Mg1–C1: 2.2360(18); Mg1–C12: 2.2554(18); Mg1–C23: 2.2434(18); Mg1–Br1: 2.4934(6); C1–Mg1–C12: 113.16(6); C1–Mg1–C23: 107.38(6); C1–Mg1–Br1: 107.99(5); C12–Mg1–C23: 111.00(7); C12–Mg1–Br1: 107.93(5); C23–Mg1–Br1: 109.29(5).

Spectral Data

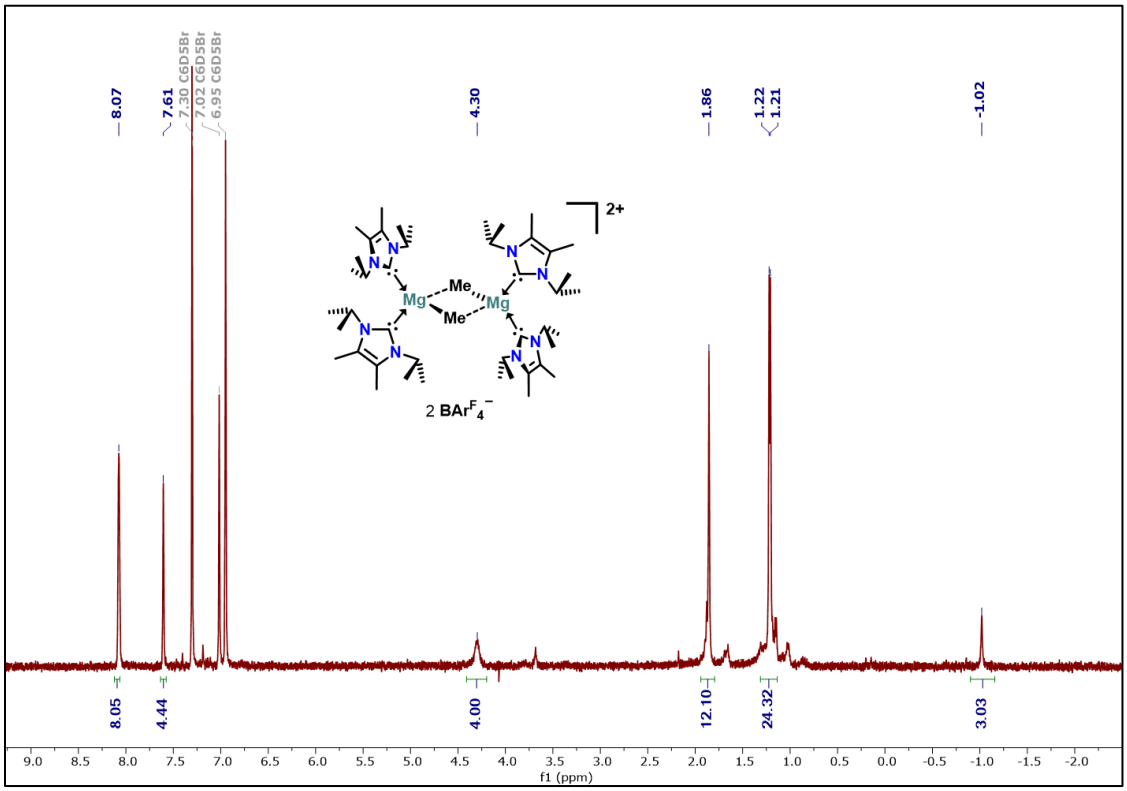

Figure S3: ^{1}H NMR spectrum (500 MHz, C_6D_5Br, 398 K) of **2**.

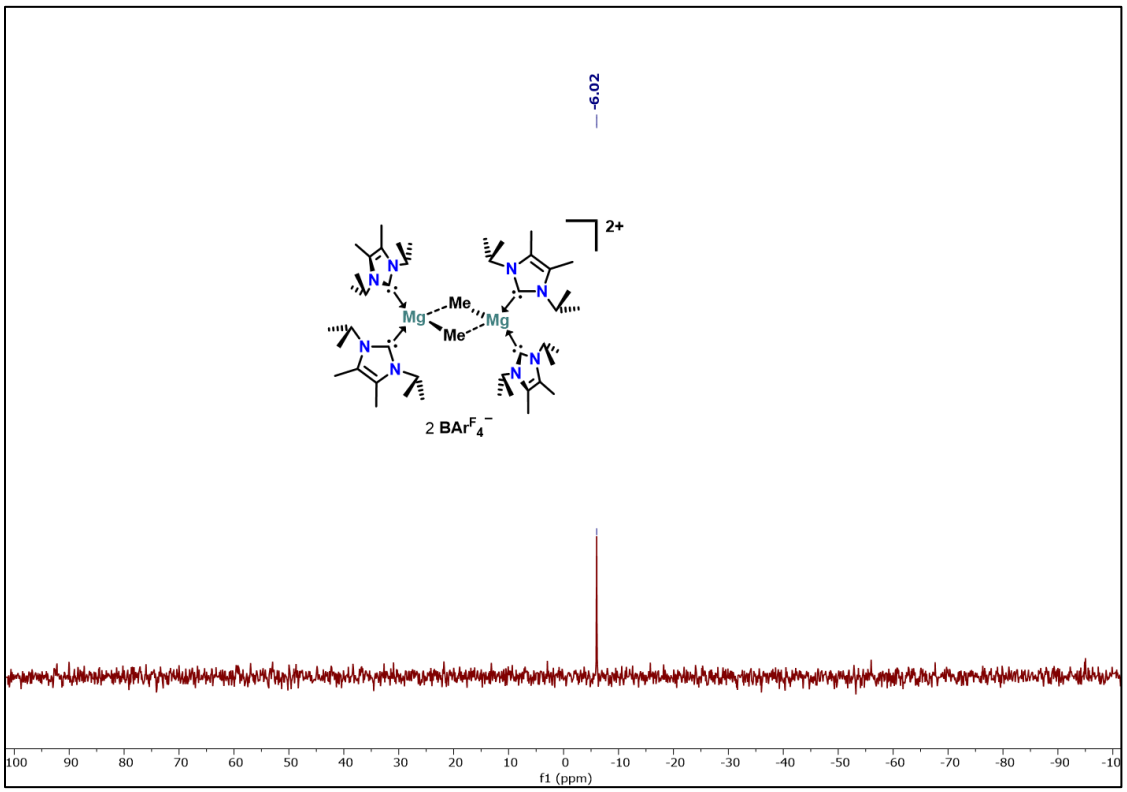

Figure S4: ^{11}B NMR spectrum (192.55 MHz, C_6D_5Br, 298 K) of **2**.

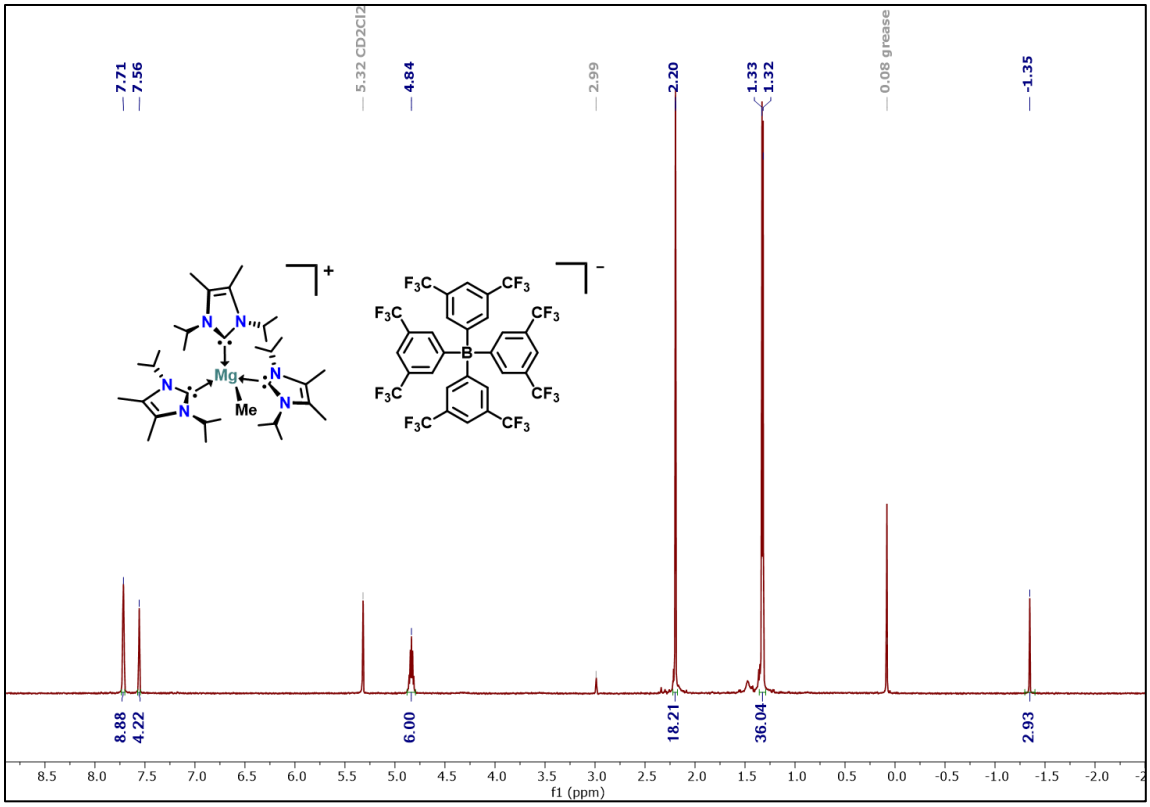

Figure S5: ^{1}H NMR spectrum (600 MHz, CD_2Cl_2, 298 K) of **3[BAr$^{F}_{4}$]**.

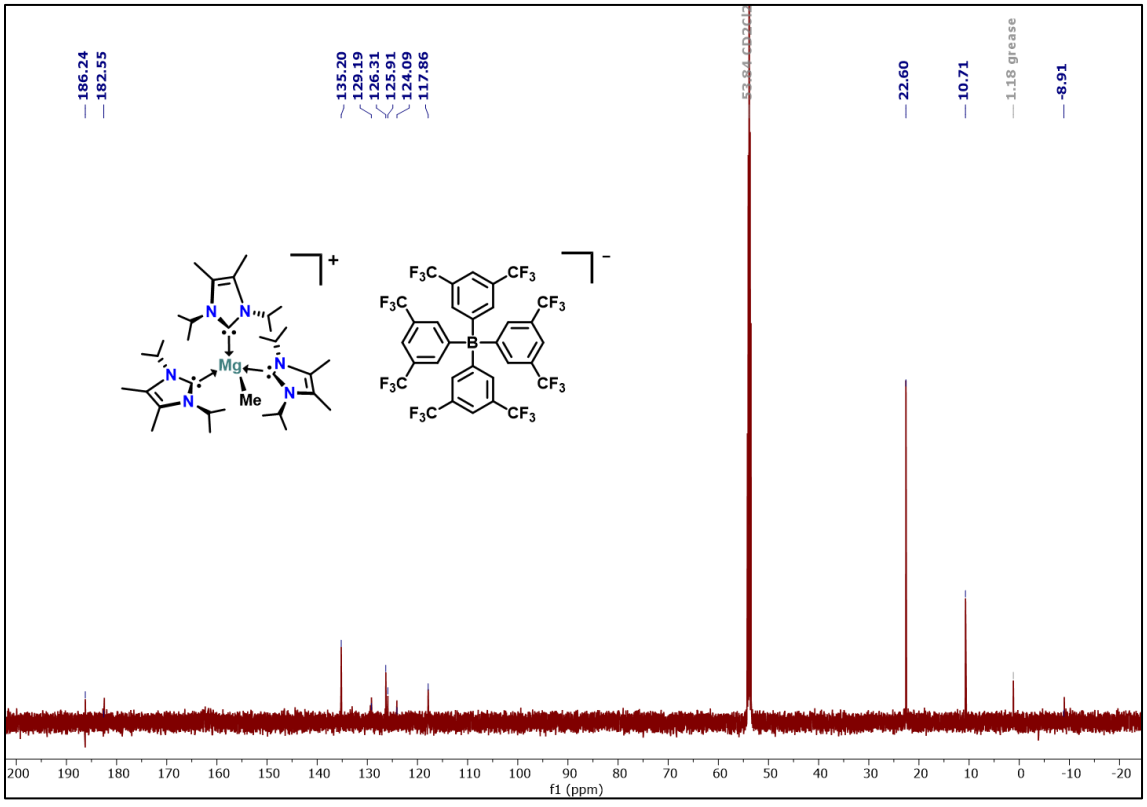

Figure S6: $^{13}C\{^{1}H\}$ NMR spectrum (151 MHz, CD_2Cl_2, 298 K) of **3[BAr$^{F}_{4}$]**.

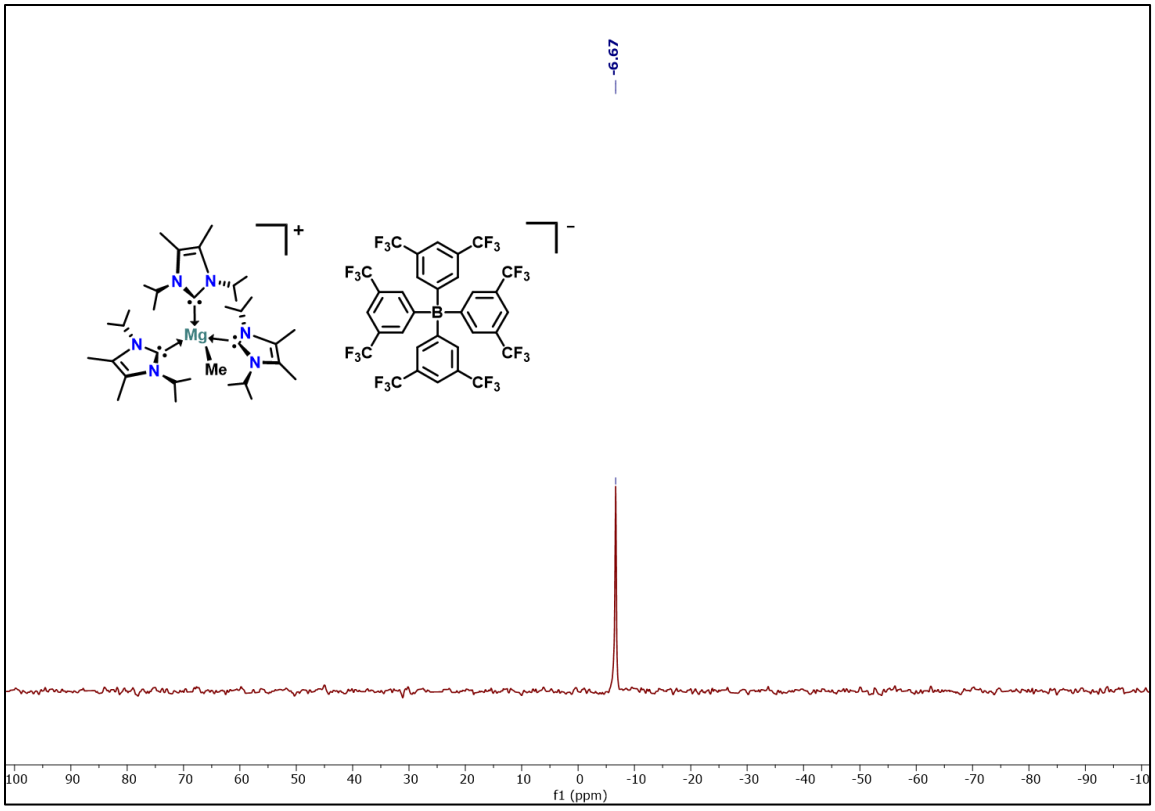

Figure S7: ^{11}B NMR spectrum (192.55 MHz, CD_2Cl_2, 298 K) of **3[BAr$^F_4$]**.

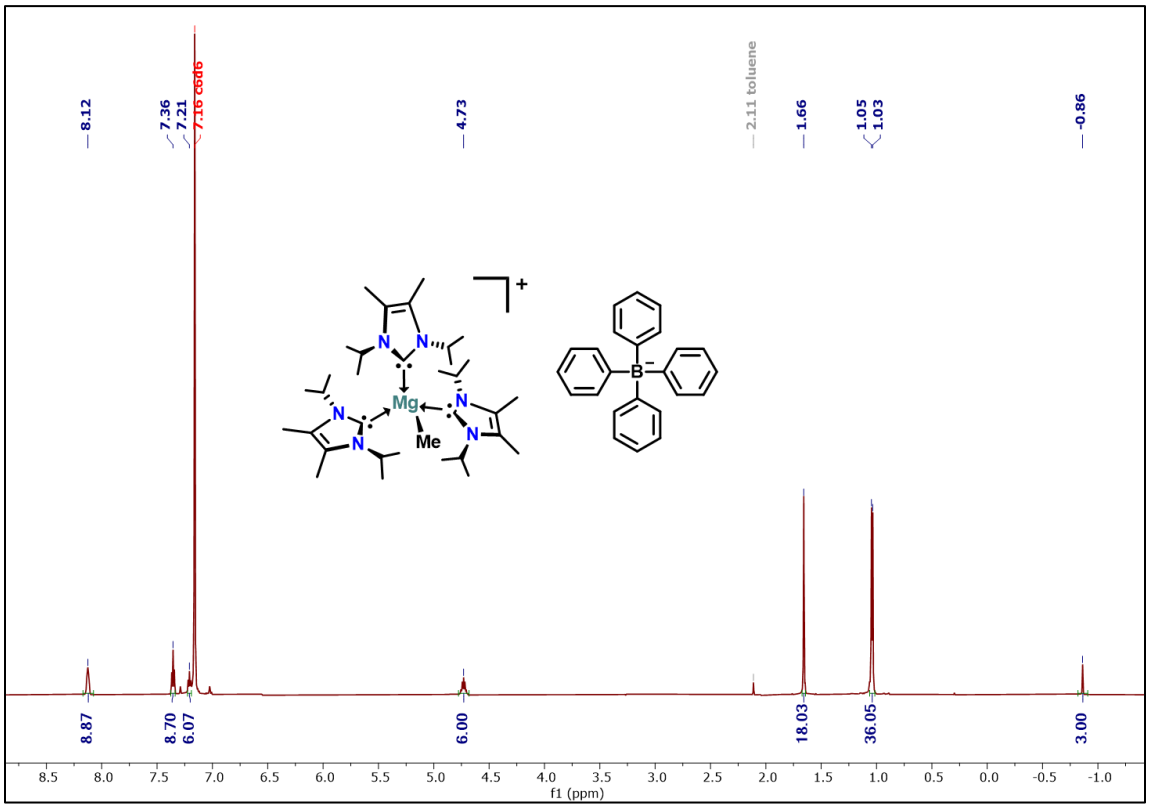

Figure S8: ^{1}H NMR spectrum (600 MHz, C_6D_6, 298 K) of **3[BPh$_4$]**.

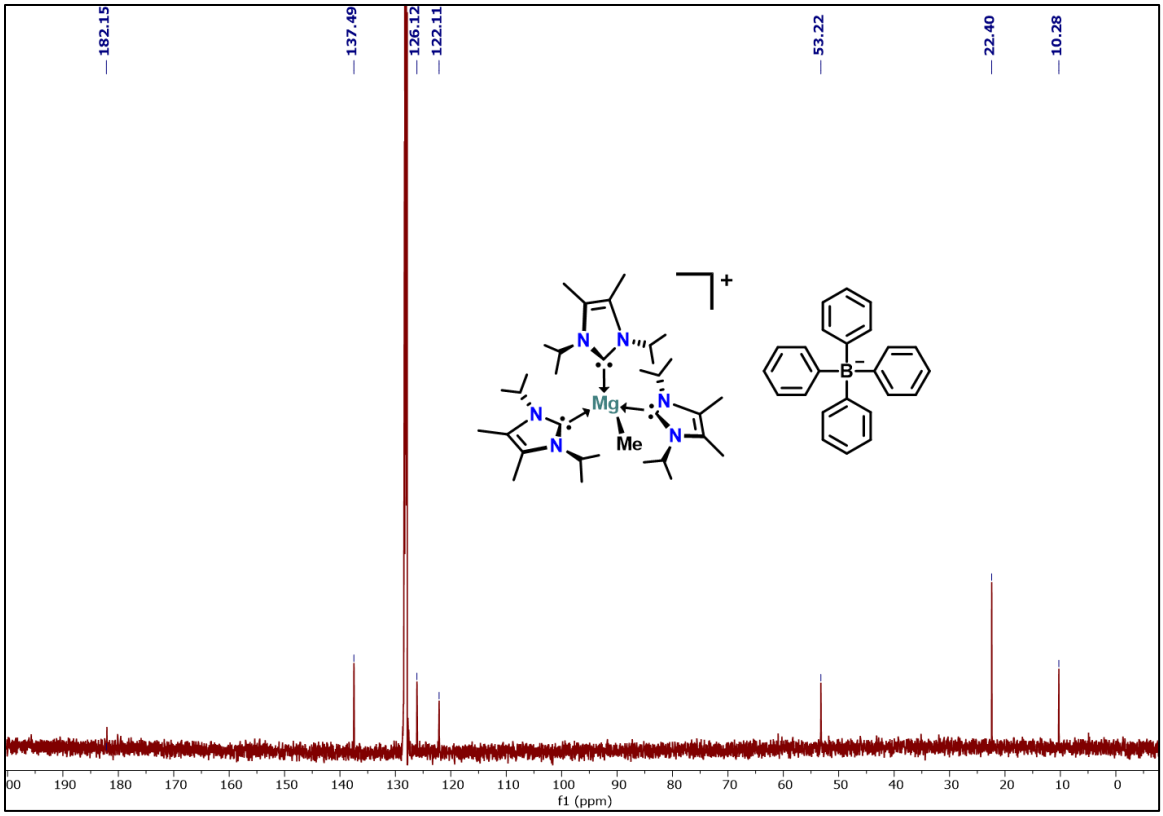

Figure S9: $^{13}C\{^{1}H\}$ NMR spectrum (151 MHz, C_6D_6, 298 K) of **3[BPh$_4$]**.

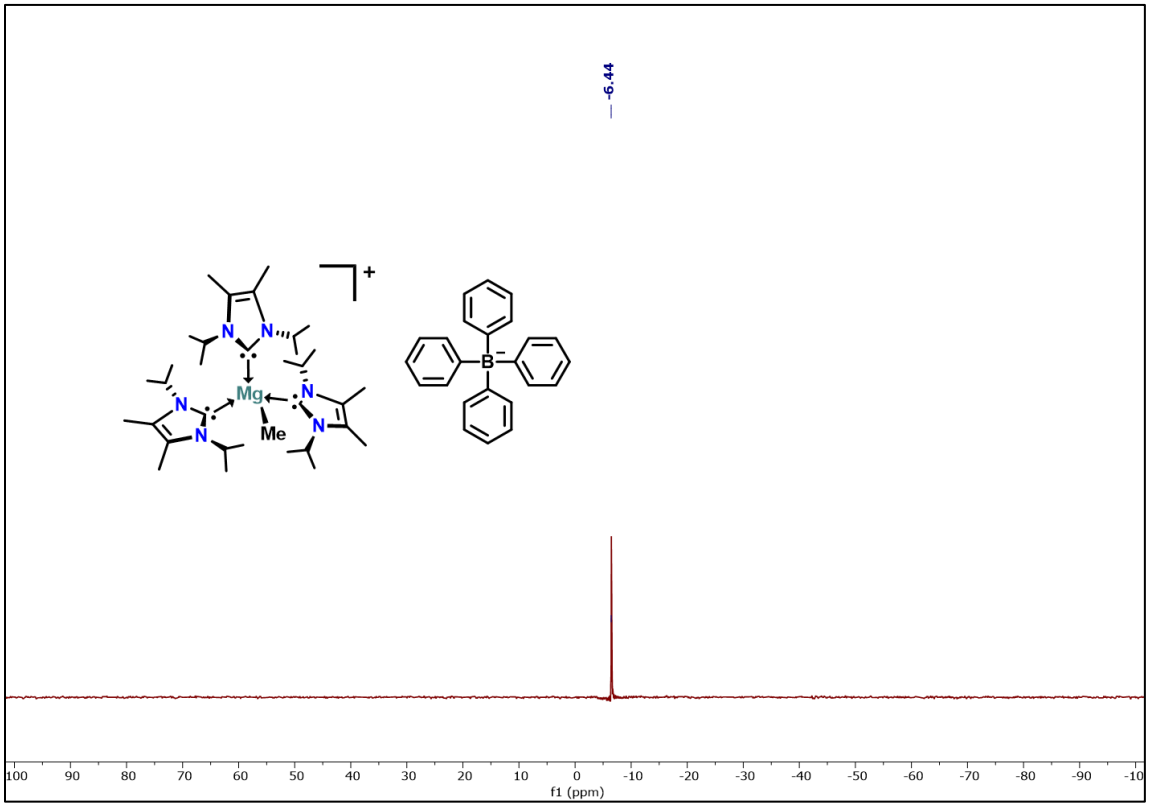

Figure S10: ^{11}B NMR spectrum (192.55 MHz, CD_2Cl_2, 298 K) of **3[BPh$_4$]**.

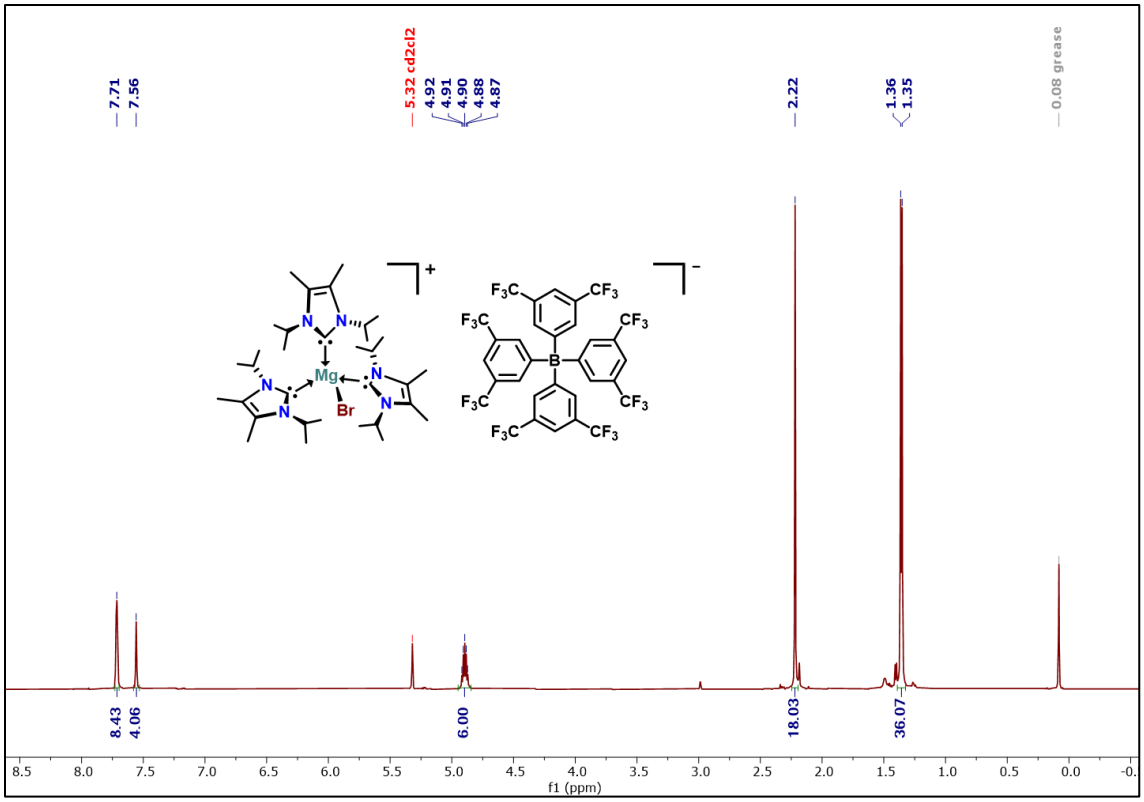

Figure S11: ^{1}H NMR spectrum (600 MHz, CD_2Cl_2, 298 K) of **4[BAr$^{F}_{4}$]**.

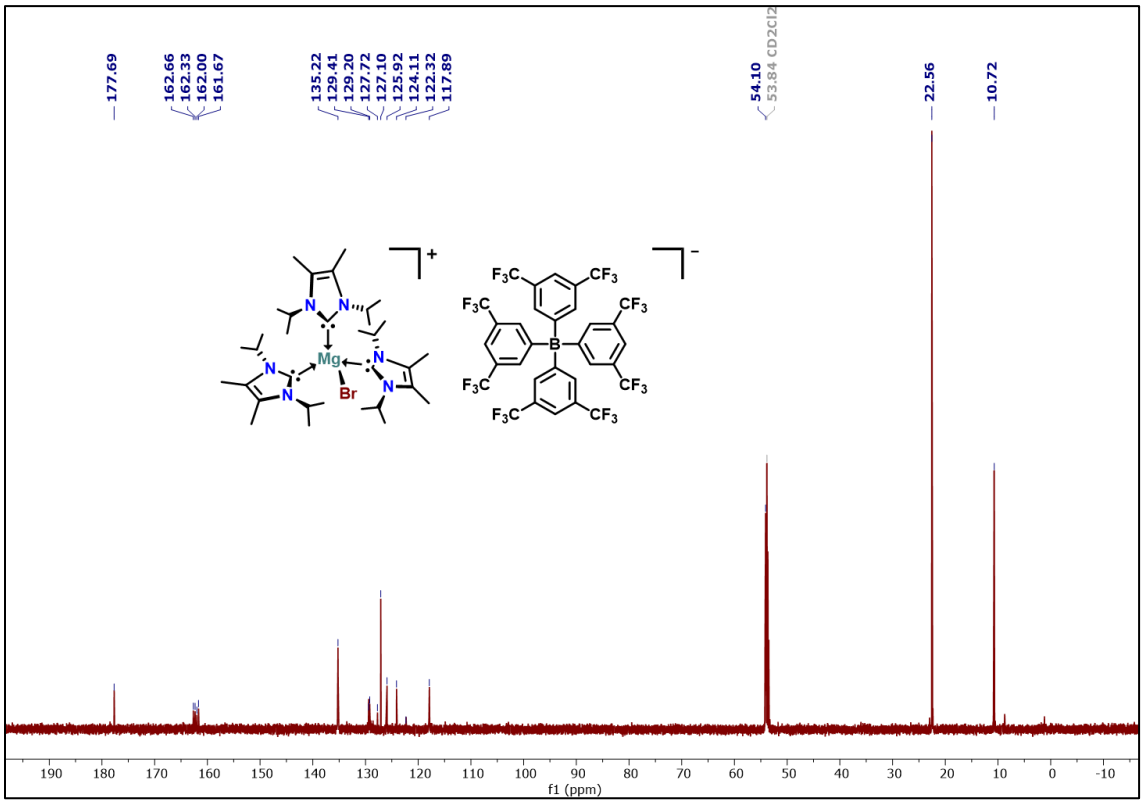

Figure S12: $^{13}C\{^{1}H\}$ NMR spectrum (151 MHz, CD_2Cl_2, 298 K) of **4[BAr$^{F}_{4}$]**.

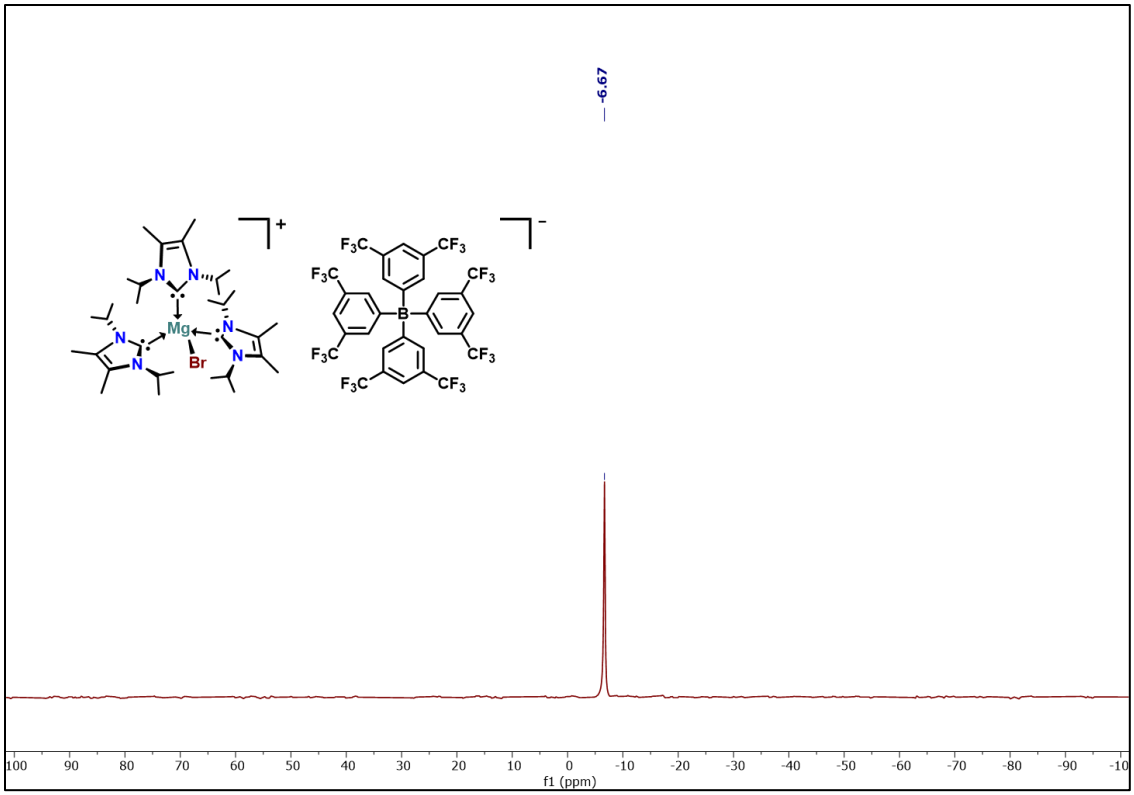

Figure S13: ^{11}B NMR spectrum (192.55 MHz, CD_2Cl_2, 298 K) of **4[BAr$^F_4$]**.

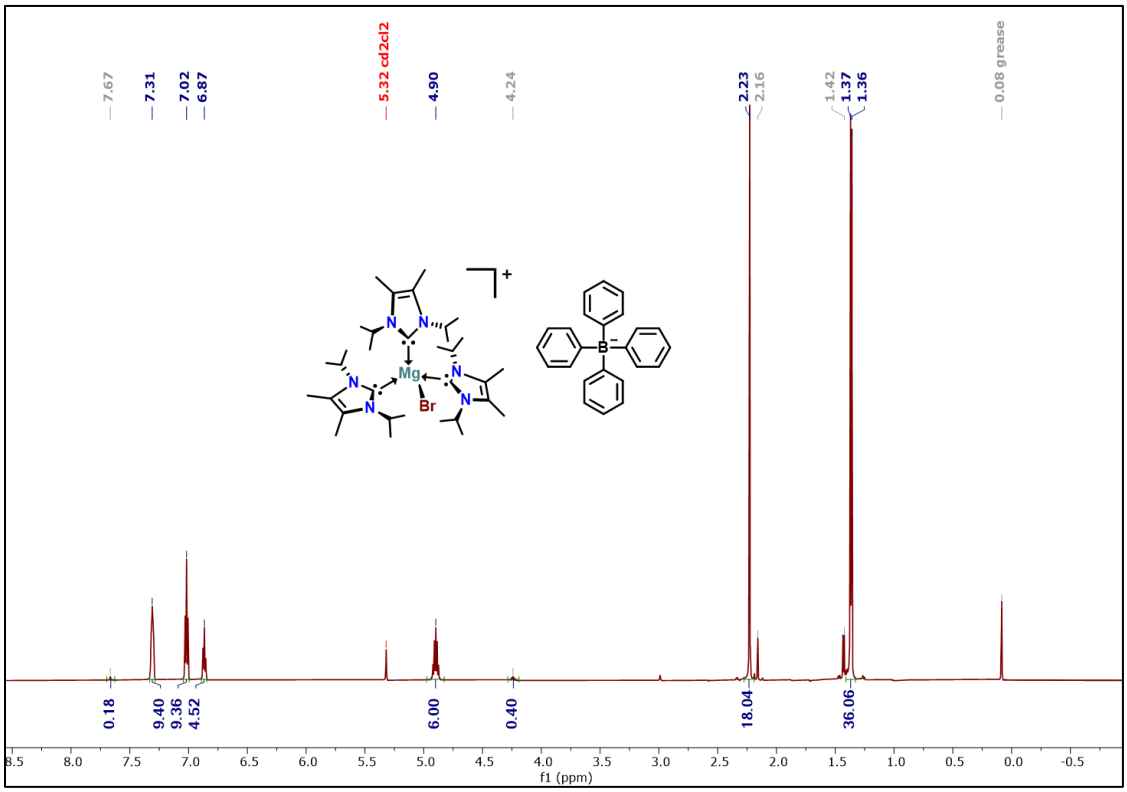

Figure S14: ^1H NMR spectrum (600 MHz, CD_2Cl_2, 298 K) of **4[BPh$_4$]**. Unlabeled peaks in grey represent hydrolysis product.

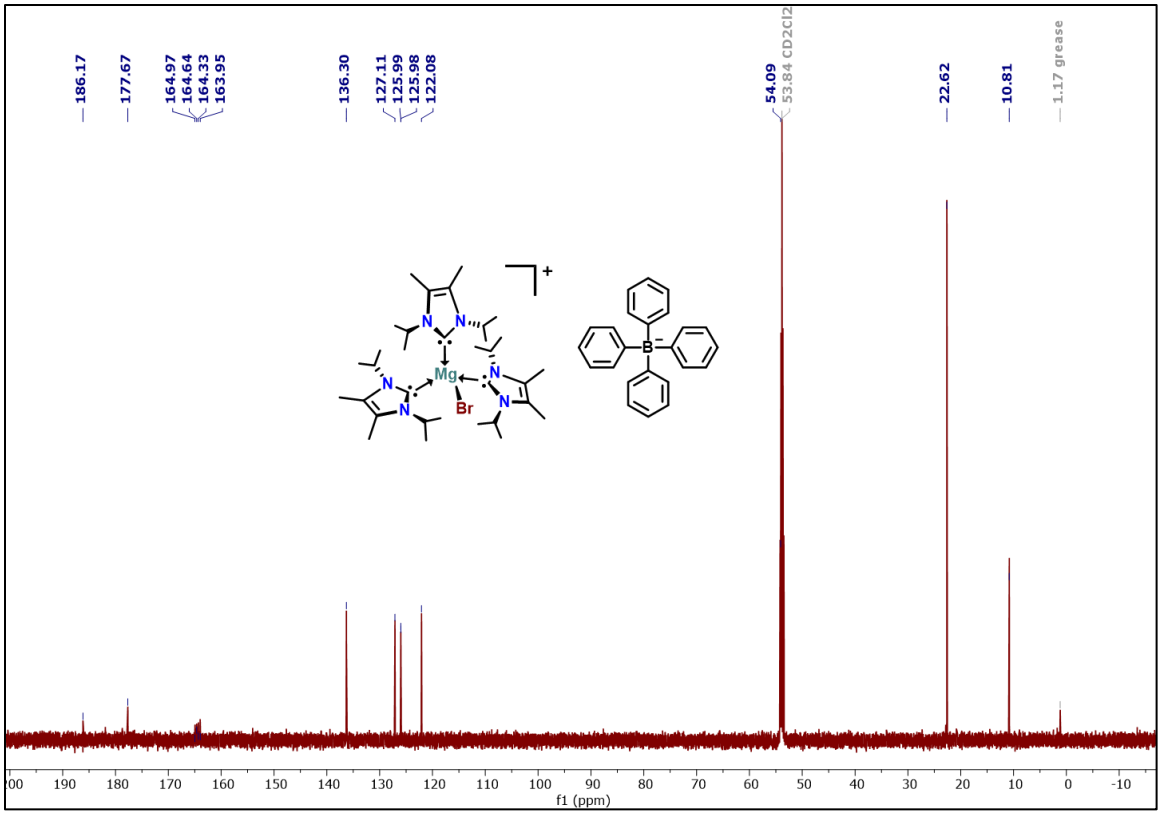

Figure S15: $^{13}C\{^{1}H\}$ NMR (151 MHz, CD_2Cl_2, 298 K) of **4[BPh$_4$]**.

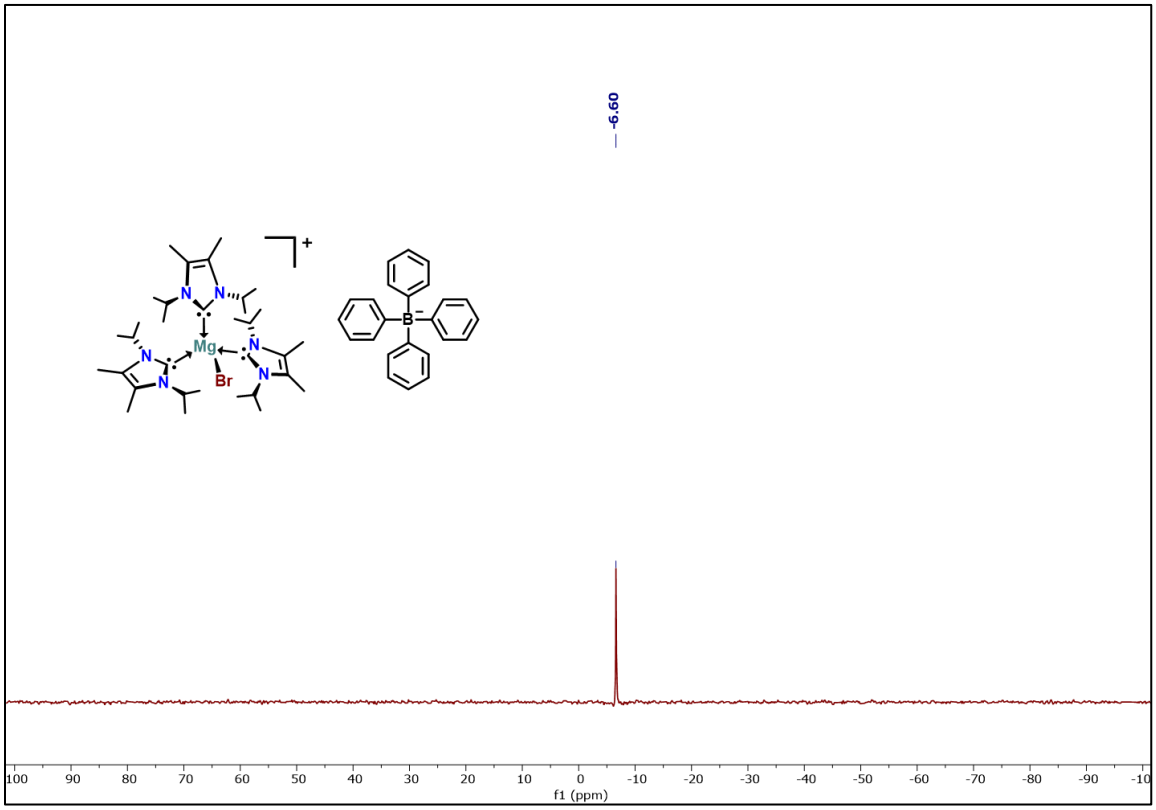

Figure S16: ^{11}B NMR spectrum (192.55 MHz, CD_2Cl_2, 298 K) of **4[BPh$_4$]**.

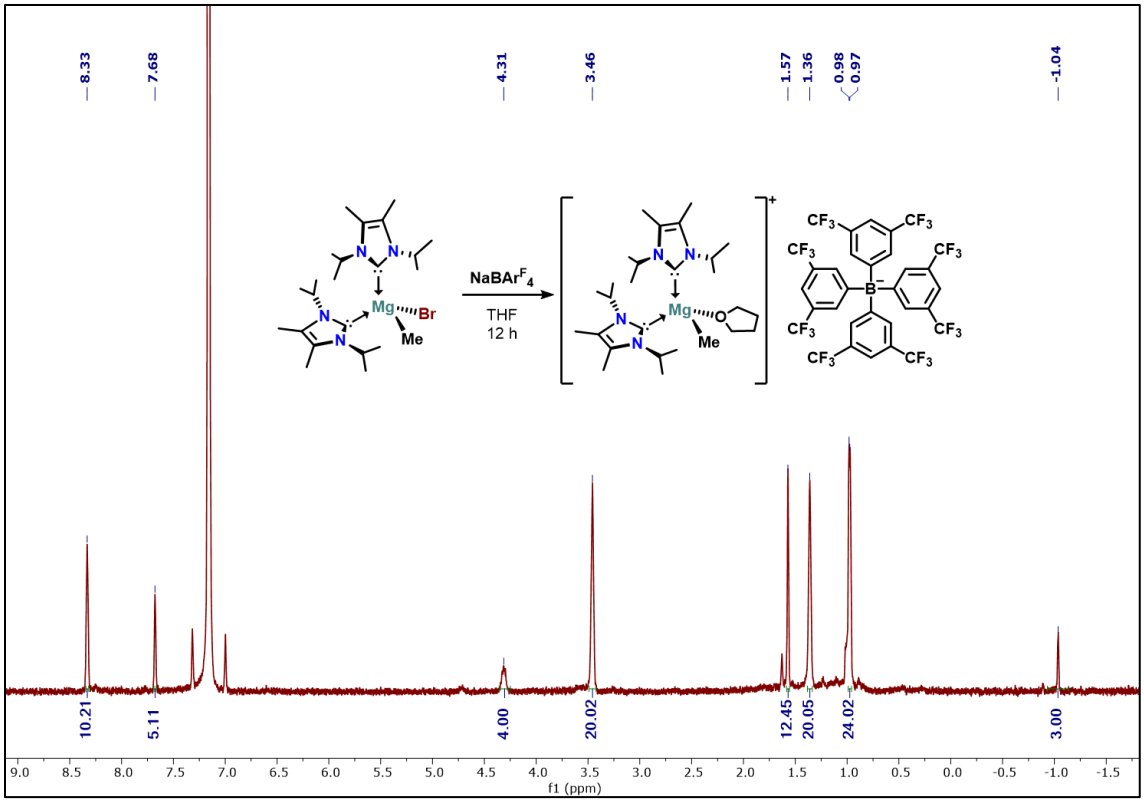

Figure S17: ^{1}H NMR spectrum (600.13 MHz, C_6D_6, 298 K) of **5[BAr$^F_4$]**.

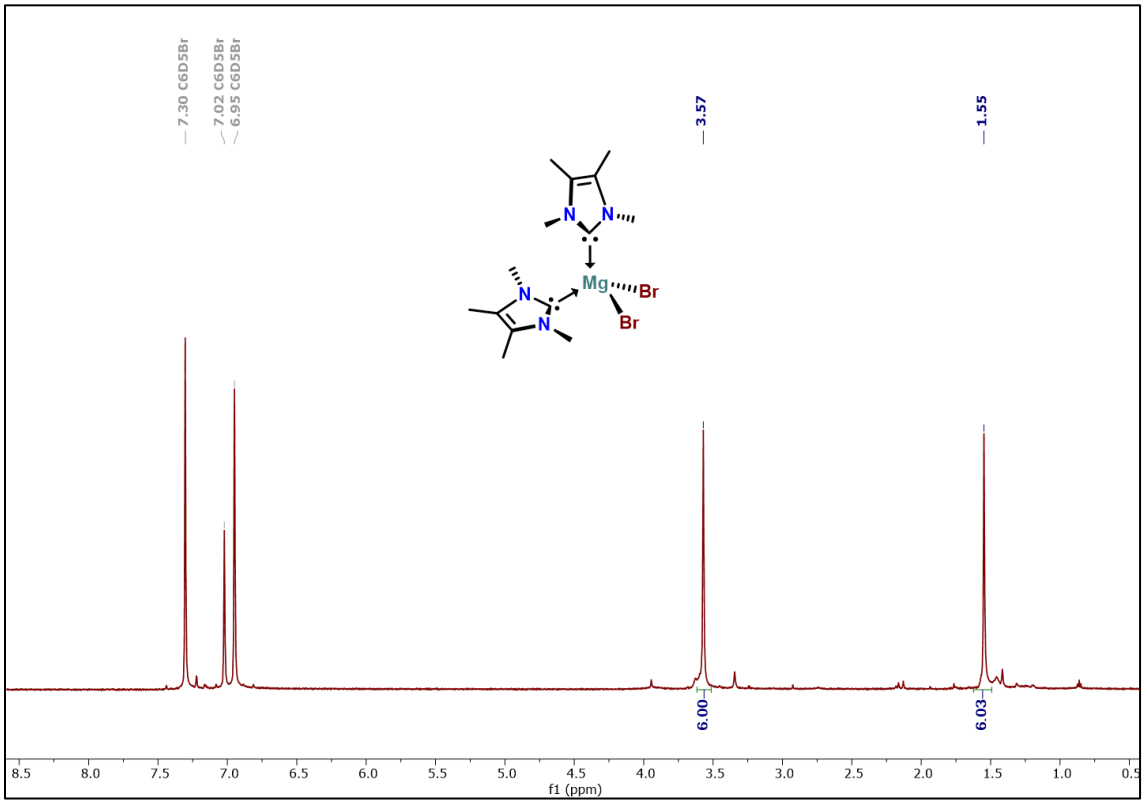

Figure S18: ^{1}H NMR spectrum (600.13 MHz, C_6D_5Br, 298 K) of **7**.

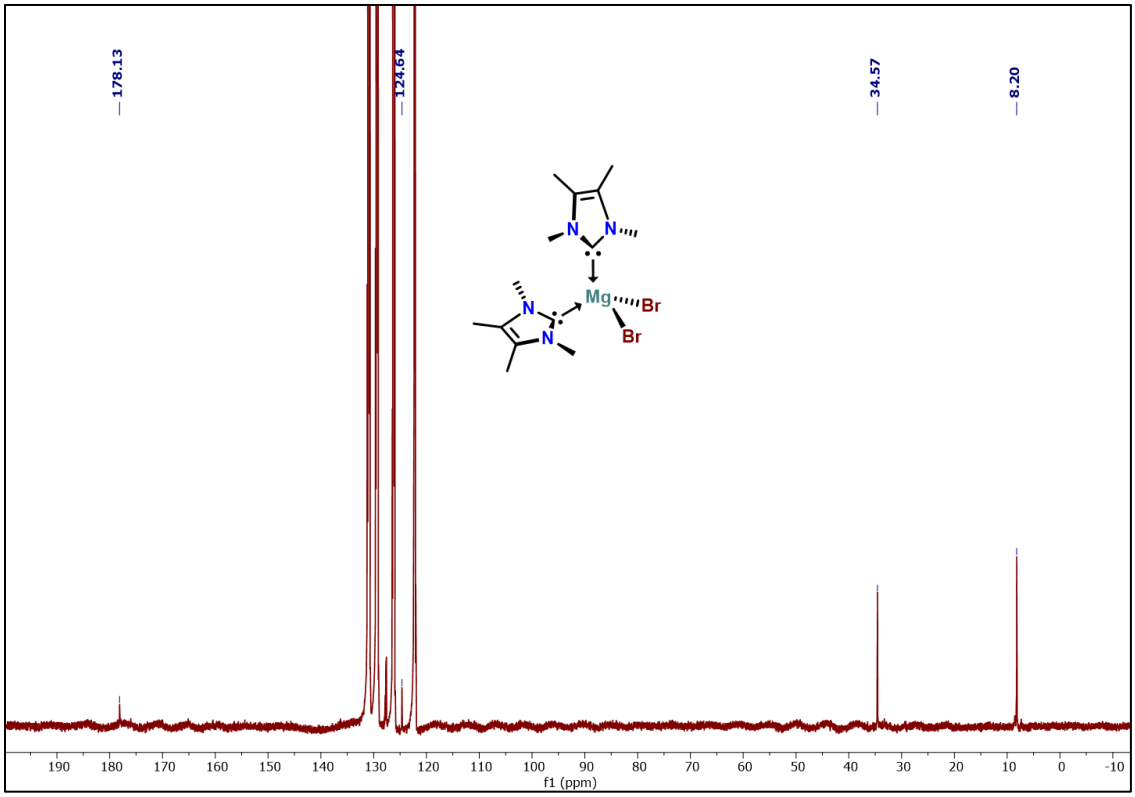

Figure S19: $^{13}C\{^{1}H\}$ NMR spectrum (200 MHz, C_6D_5Br, 298 K) of **7**.

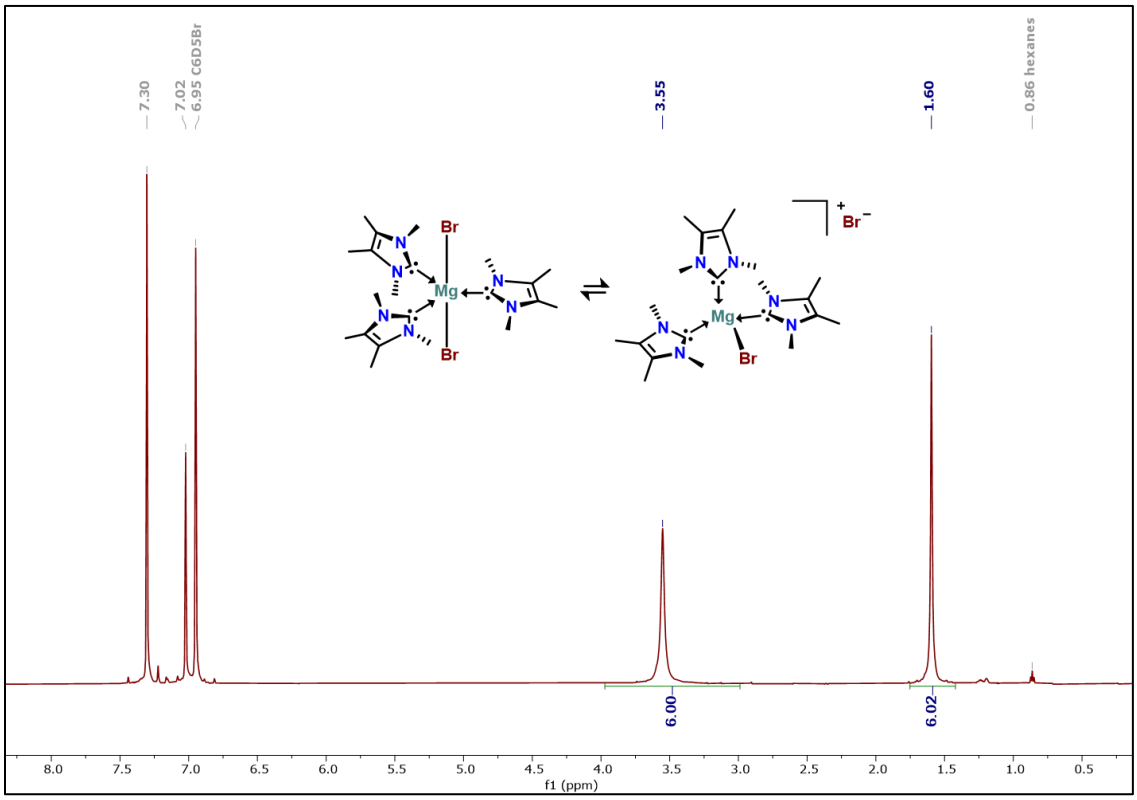

Figure S20: ^{1}H NMR spectrum (600.13 MHz, C_6D_5Br, 298 K) of **8**.

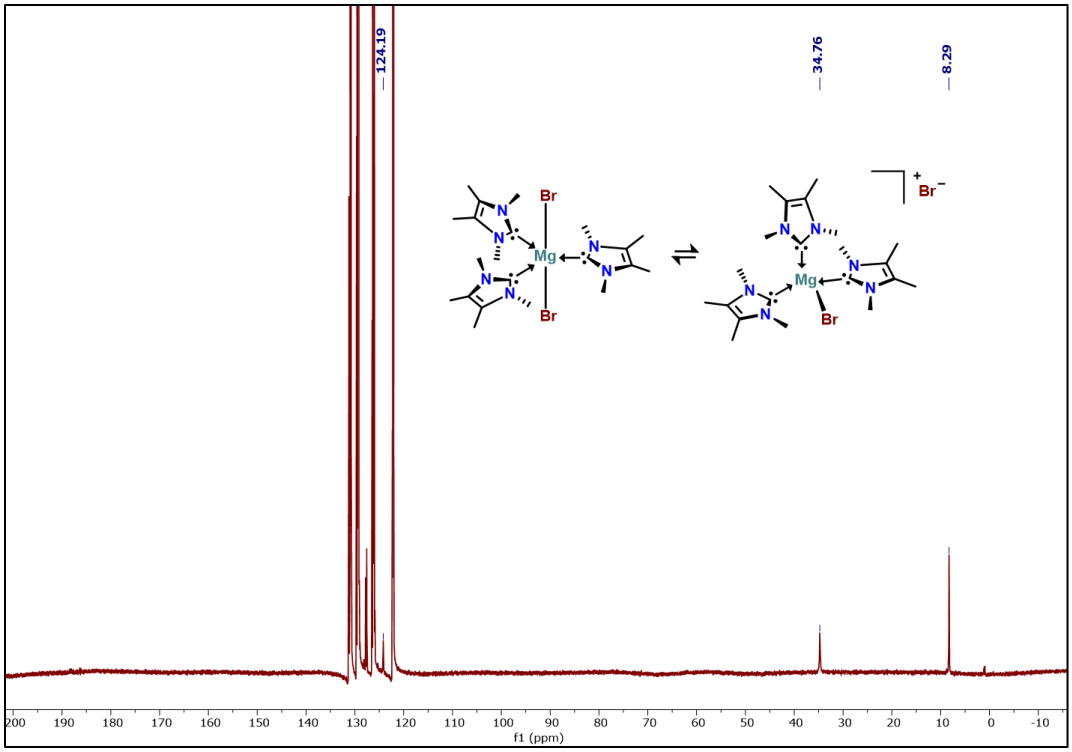

Figure S21: $^{13}C\{^{1}H\}$ NMR spectrum (200 MHz, C_6D_5Br, 298 K) of **8**.

Reactions involving Ligand rearrangement products. ^{1}H NMR spectrum (600 MHz, CD_2Cl_2, 298 K) described unless otherwise indicated.

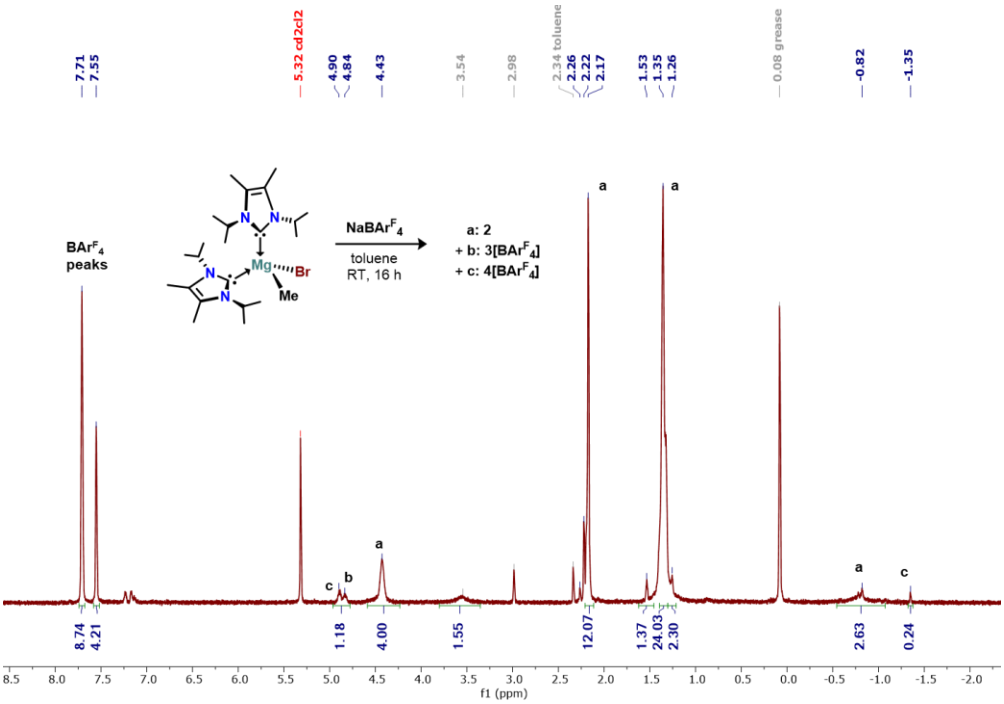

Figure S22: Reaction of **1** and $Na[BAr^F_4]$ in toluene.

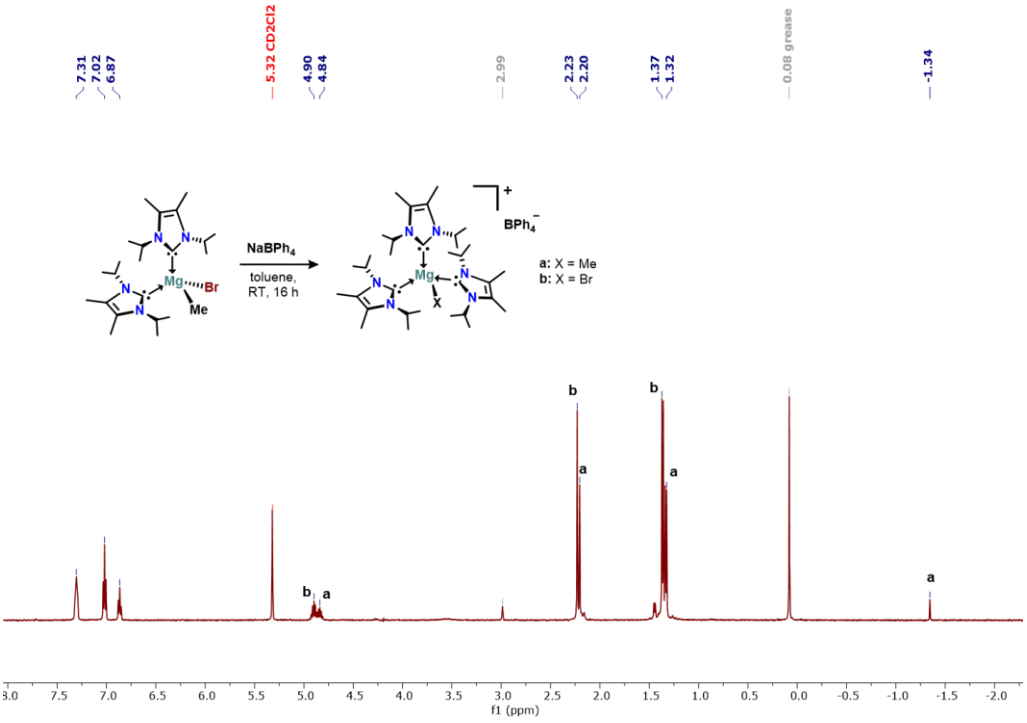

Figure S23: Reaction of **1** and $Na[BPh_4]$ in toluene.

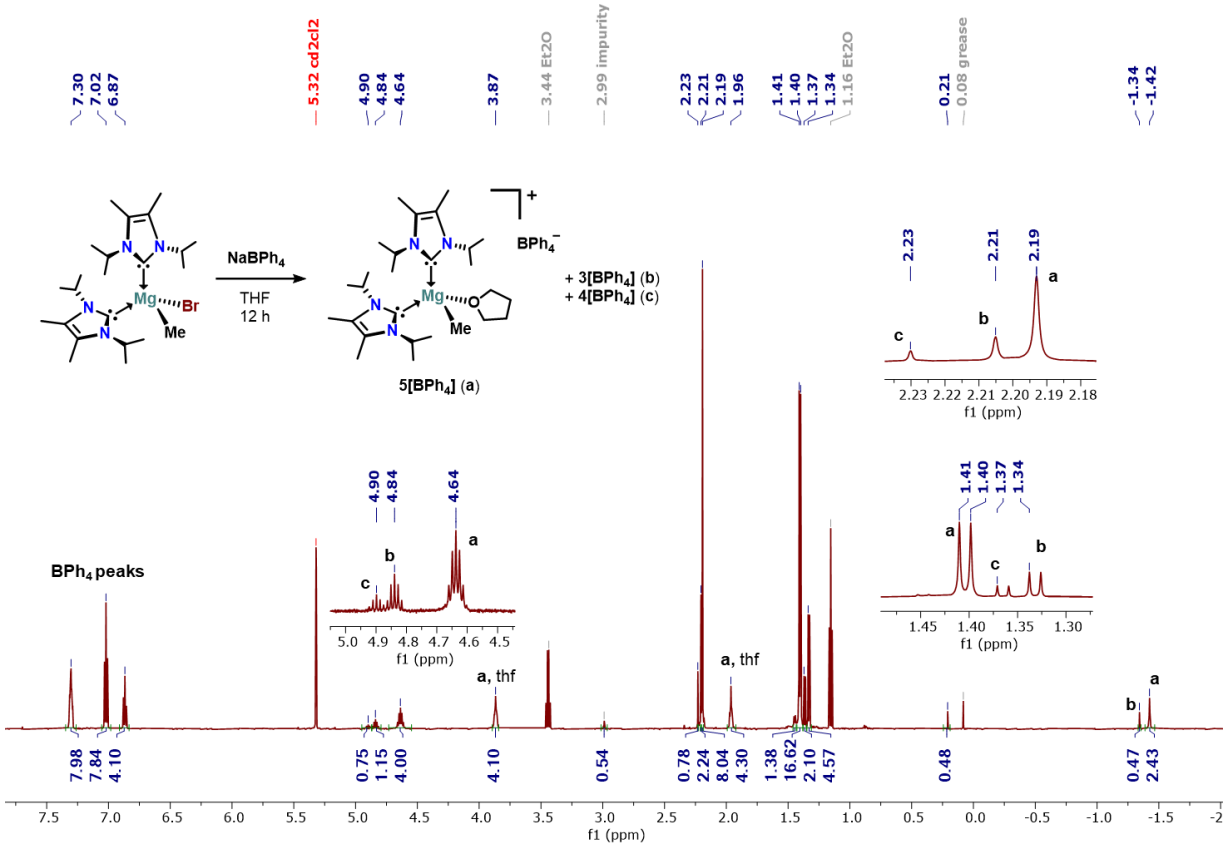

Figure S24: Synthesis of **5[BPh$_4$]**.

Crystallographic Refinement Details

General Considerations.

A suitable single crystal of each complex was was coated with Paratone oil and mounted on a MiTeGen MicroLoop. The X-ray intensity data were measured on a Bruker Kappa APEXII Duo system. The Incoatec Microfocus IμS (Cu K_α, λ = 1.54178 Å) and a multi-layer mirror monochromator were used for **2**, **3[BAr$^F_4$]**, **4[BAr$^F_4$]**, **5[BPh$_4$]**, and **8**, and the fine-focus sealed tube (Mo K_α, λ = 0.71073 Å) and a graphite monochromator were used for **3[BPh$_4$]**, **4[BPh$_4$]**, and **7**. The frames were integrated with the Bruker SAINT software package[1] using a narrow-frame algorithm. Data were corrected for absorption effects using the Multi-Scan method (SADABS).[1] Each structure was solved and refined using the Bruker SHELXTL Software Package[2] within APEX3[1] and OLEX2.[3] Non-hydrogen atoms were refined anisotropically. Hydrogen atoms were placed in geometrically calculated positions with U_{iso} = 1.2U_{equiv} of the parent atom (U_{iso} = 1.5U_{equiv} for methyl) unless otherwise specified below.[1]

In **2**, the best available crystal diffracted extremely weakly and it was not possible to collect data to the typical resolution. Nevertheless, enough data was obtained to unambiguously determine the connectivity of the structure. The C-H hydrogen atoms of the bridging methyl groups were located in the diffraction map and refined isotropically with U_{iso} = 1.5U_{equiv} of the parent carbon and restraints on the bond distances. Several sites of disorder were identified in the structure. The relative occupancies of each disordered site was freely refined, and constraints and restraints were used as needed on the anisotropic displacement parameters and/or the bond lengths of the disordered atoms.

In **3[BPh$_4$]**, both the cation and anion were extensively disordered. The relative occupancies of the disordered sites was freely refined. Constraints were used on the anisotropic displacement parameters of one disordered phenyl and one disordered imidazole. Constraints were also used on the bond lengths of the minor position of one disordered phenyl.

In **4[BAr$^F_4$]**, one CF_3 group was extremely disordered by rotation. It was modeled over three positions with the sum set to 1 and with constraints on the anisotropic displacement parameters of the disordered atoms.

In **5[BPh$_4$]**, the relative occupancies of the methyl and Br substituents was freely refined, and constraints were used on the anisotropic displacement parameters of the disorder atoms.

In **7**, a two-component twin was identified using CELL_NOW.[4] Starting with 1267 reflections, 1180 reflections were fit to the first domain, 1054 to the second domain (56 exclusively), with 31 unindexed reflection remaining. The twin domain was oriented at a 179.8º rotation about the reciprocal axis 0.004 0.000 1.000. The twin law was -0.996 0.003 0.008 / -0.006 -1.000 0.000 / 1.042 0.000 0.996. The structure was refined on HKLF5 data, with the BASF for the twin domains refining to 0.40527.

Table S1. Crystallographic details for compounds **2**-**5** and **7**-**8**.

	2	**3[BPh$_4$]**	**3[BAr$^F_4$]**	**4[BPh$_4$]**	**4[BAr$^F_4$]**	**5[BPh$_4$]**	**7**	**8**
CCDC number	1998358	1998359	1998360	1998361	2018107	1998362	1998363	1998364
Formula	$C_{116}H_{115}B_2ClF_{48}Mg_2N_8$	$C_{58}H_{83}BMgN_6$	$C_{66}H_{75}BF_{24}MgN_6$	$C_{57}H_{80}BBrMgN_6$	$C_{65}H_{72}BBrF_{24}MgN_6$	$C_{50.95}H_{70.84}BBr_{0.06}MgN_4O$	$C_{14}H_{24}Br_2MgN_4$	$C_{42}H_{72}Br_4Mg_2N_{12}$
FW (g/mol)	2638.84	899.42	1443.44	964.30	1508.45	794.81	432.50 g/mol	1113.37
Temp (K)	100(2)	100(2)	100(2)	100(2)	100(2)	100(2)	100(2) K	100(2)
λ (Å)	1.54178	0.71073	1.54178	0.71073	0.71073	1.54178	0.71073 Å	1.54178
Size (mm)	0.045 x 0.119 x 0.126	0.354 x 0.357 x 0.420	0.041 x 0.136 x 0.211	0.092 x 0.101 x 0.189	0.182 x 0.412 x 0.697	0.009 x 0.092 x 0.17	0.160 x 0.172 x 0.332 mm	0.103 x 0.106 x 0.121
Crystal habit	colorless plate	colorless block	colorless plate	colorless rod	colorless block	colorless plate	colorless plate	colorless block
Crystal system	triclinic	monoclinic	monoclinic	monoclinic	monoclinic	triclinic	monoclinic	cubic
Space group	P -1	P 2_1/c	P 2_1/n	P 2_1/n	P 2_1/n	P -1	P 2_1/n	P 2_1 3
a (Å)	18.4203(19)	17.4055(8)	13.2568(8)	13.6535(9)	13.3434(13)	10.2417(10)	9.330(3)	17.1849(3)
b(Å)	18.6215(13)	16.3293(7)	29.5926(19)	18.0955(11)	29.497(3)	15.0602(14)	13.996(4)	17.1849(3)
c (Å)	20.3747(15)	20.5763(10)	18.5731(11)	22.0243(14)	18.5791(16)	15.7584(15)	14.737(6)	17.1849(3)
α (°)	81.055(4)	90	90	90	90	85.263(7)	90	90
β (°)	71.991(6)	111.0440(10)	104.157(4)	91.008(2)	104.397(3)	77.588(7)	107.376(10)	90
γ (°)	68.409(4)	90	90	90	90	81.071(7)	90	90
Volume (Å^3)	6173.2(9)	5458.1(4)	7065.0(8)	5440.6(6)	7082.9(11)		1836.6(11)	5075.1(3)
Z	2	4	4	4	4	2	4	4
Density (g/cm^3)	1.420	1.095	1.357	1.177	1.415	1.127	1.564 g/cm^3	1.457
μ (mm^{-1})	1.469	0.074	1.168	0.808	0.696	0.677	4.447 mm^{-1}	4.439
F(000)	2700	1960	2984	2064	3088	863	872	2288
θ range (°)	2.28 to 58.31	1.25 to 25.39	2.87 to 68.76	1.74 to 25.71	1.32 to 27.57	2.88 to 68.63	2.05 to 26.44°	3.64 to 68.13
Index ranges	-20 ≤ h ≤19 -20 ≤ k ≤ 20 -22 ≤ l ≤ 22	-21 ≤ h ≤ 20 -19 ≤ k ≤ 19 -24 ≤ l ≤ 16	-14 ≤ h ≤ 15 -35 ≤ k ≤ 35 -22 ≤ l ≤ 22	-16 ≤h ≤ 16 -19 ≤ k ≤ 22 -26 ≤ l ≤ 26	-17 ≤ h ≤ 17 -38 ≤ k ≤ 36 -23 ≤ l ≤ 24	-10 ≤h ≤ 12 -18 ≤ k ≤18 -18 ≤ l ≤ 18	-11 ≤h ≤ 11 0 ≤ k ≤17 0 ≤ l ≤ 18	-20 ≤h ≤ 12 -14 ≤ k ≤ 20 -19 ≤ l ≤ 19
Independent refIns	17206 [R_{int} = 0.1425]	10035 [R_{int} = 0.0431]	12940 [R_{int} = 0.1640]	10347 [R_{int} = 0.1079]	16305 [R_{int} = 0.0293]	8529 [R_{int} = 0.0993]	3834[R_{int} = 0.1411]	3133 [R_{int} = 0.0605]
Data / restraints /parameters	17206 / 312 / 1655	10035 / 0 / 898	12940 / 0 / 931	10347 / 0 / 613	16305 / 109 / 958	8529/0/540	3834 / 0 / 199	3113 / 0 / 189
GOF on F^2	1.025	1.071	0.977	0.984	1.018	1.016	1.054	1.058
R_1 (I>2σ(I))	0.1399	0.0488	0.0887	0.0535	0.0362	0.0542	0.0699	0.0348
w R_2 (all data)	0.4036	0.1530	0.2802	0.0938	0.0913	0.1425	0.1917	0.0837

Computational Data

General Considerations.

The starting geometries of compounds **2**, **3**, **4**, **5**, **7**, **8a**, and **8b** were each extracted from the X-ray crystal structures. All density functional theory geometry optimizations and corresponding harmonic vibrational frequency computations were carried out using Gaussian 16 Revision B.01[5] at the ωB97X-D/BS1 level of theory.[6] The default pruned UltraFine integration grids were used for all energy computations (99 radial shells with 590 points per shell (99,590) and pruned SG1 grids using 50 radial shells with 194 points per shell (50,194) for Hessians. The default SCF convergence criteria (10^{-8}) was used. The basis set (designated as BS1) utilized cc-pVDZ for Mg, C, O, N, and H and cc-pVDZ-PP for Br).[7] For each compound, the Wiberg bond indices (WBI) formulated within the natural atomic orbital (NAO) basis and natural charges were calculated using NBO 3.1, as implemented in Gaussian 09 Revision D.01.[8] Localized molecular orbitals were computed using Multiwfn[9] 3.7 utilizing the Pipek-Mezey[10] localization method with Mulliken population. Molecular orbitals were generated using Chemcraft (http://www.chemcraftprog.com) with a contour value of 0.05.[11]

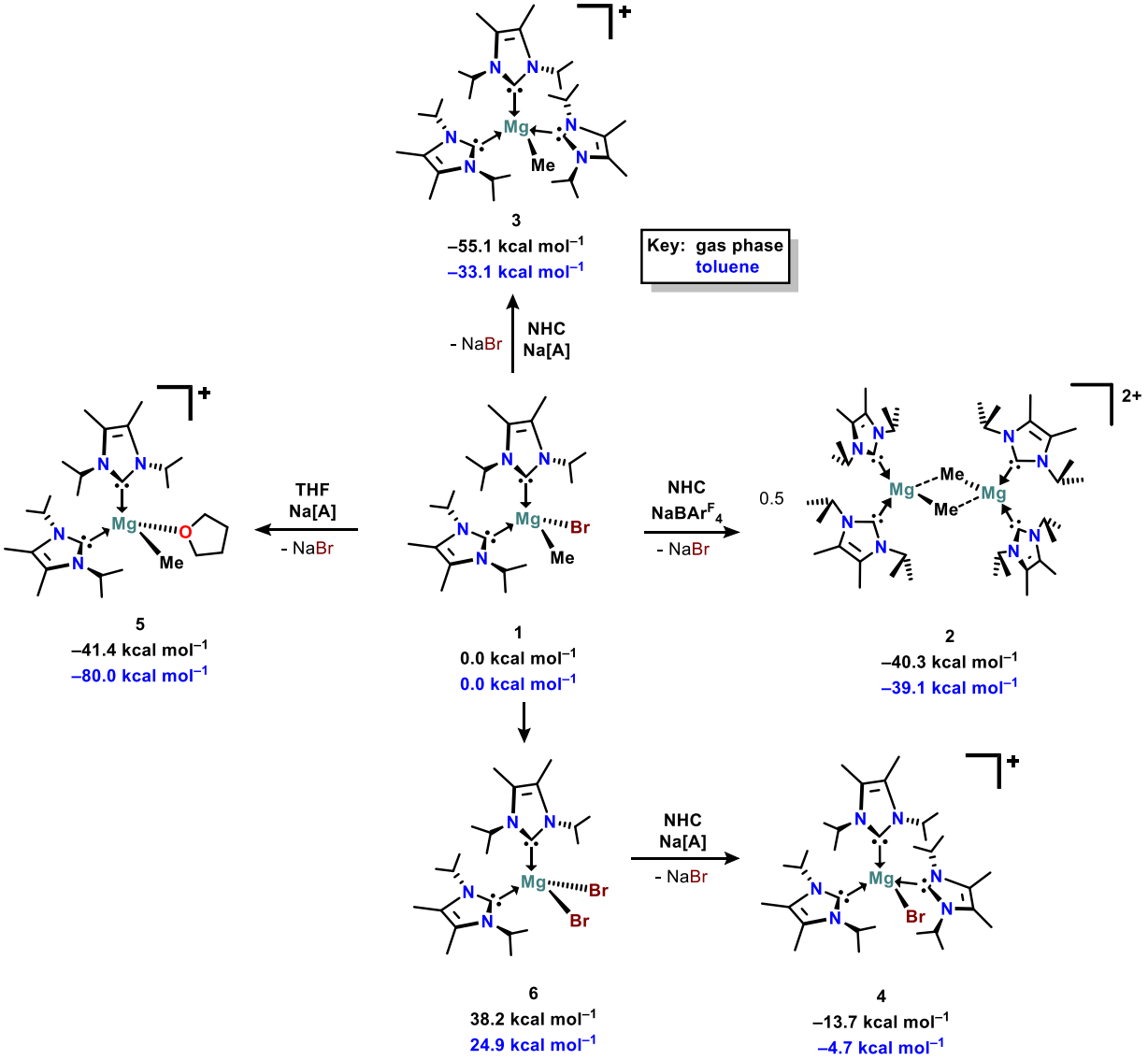

Figure S25. Energetics (ΔG) for halide abstraction reactions in gas phase (black, top) and toluene (blue, bottom).

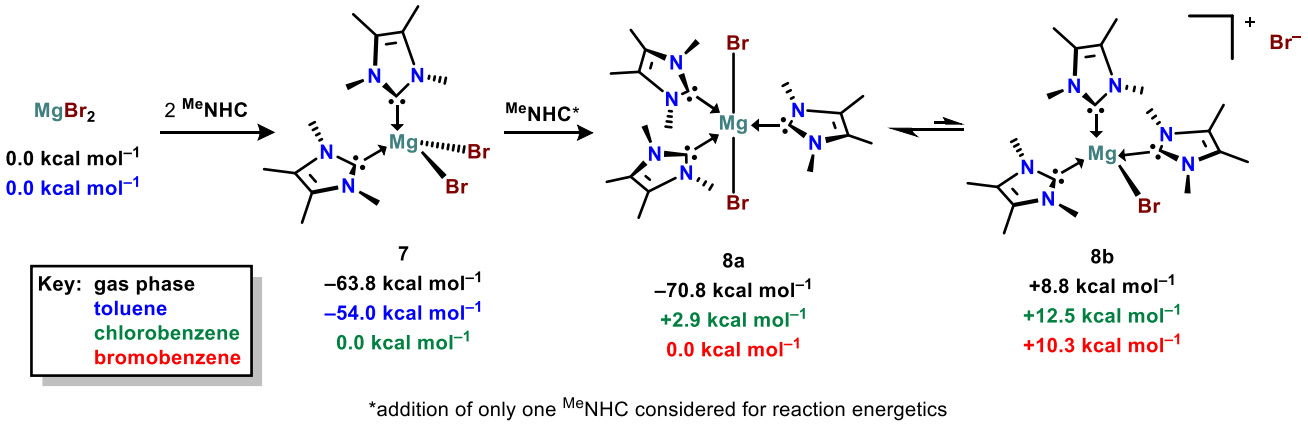

Figure S26. Energetics for $MgBr_2$ heterolysis reaction in gas phase (black), toluene (blue), chlorobenzene (green) and bromobenzene (red).

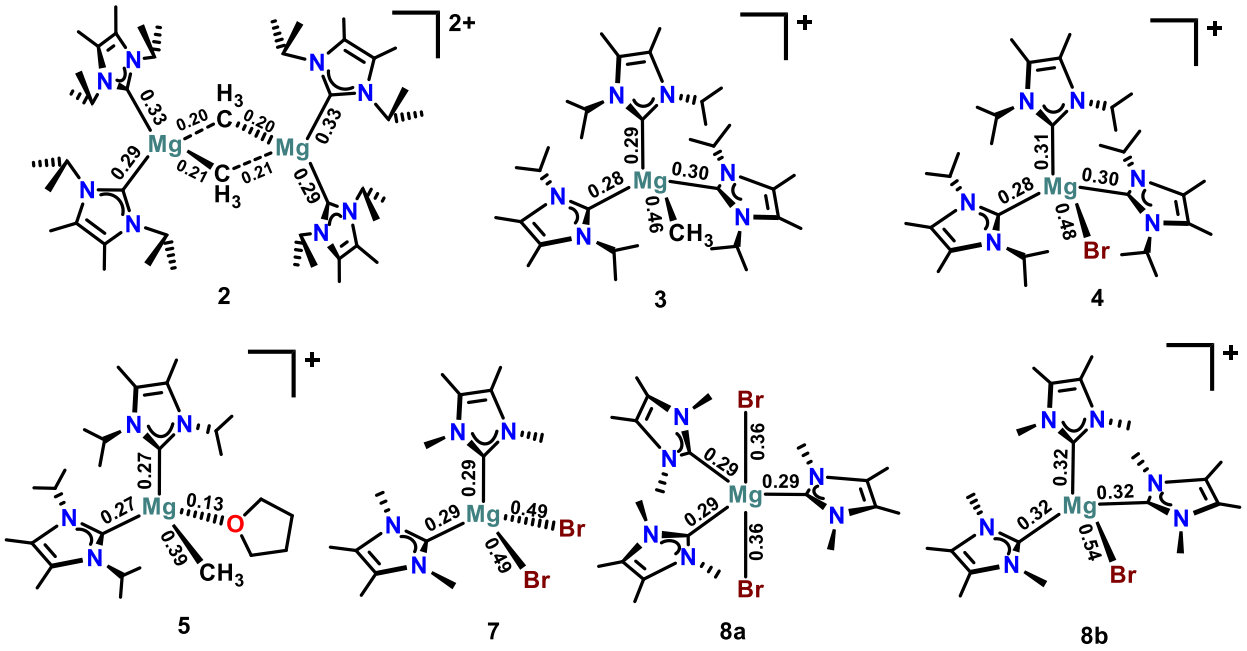

Figure S27. Isolated compounds with appropriate atoms labelled for WBI values.

Table S2. WBI and Natural Charge values for reported compounds

2^{2+} $[(^{iPr}NHC)_2Mg(\mu\text{-}Me)]_2^{2+}$ — **3^{+}** $[(^{iPr}NHC)_3Mg(Me)]^{+}$

Mg–R	R	WBI	Natural Charge	Mg–R	R	WBI	Natural Charge
	C^{1}	0.3251	0.01667		C^{1}	0.2872	0.06355
	C^{12}	0.2883	0.02710		C^{12}	0.3018	0.03134
	C^{45}	0.2016	–1.45024		C^{23}	0.2818	0.05076
	C^{46}	0.2060	–1.45024		C^{34}	0.4620	–1.19648
	Mg	–	1.26870		Mg	–	1.12977

4^{+} $[(^{iPr}NHC)_3Mg(Br)]^{+}$ — **5^{+}** $[(^{iPr}NHC)_2(THF)Mg(Me)]^{+}$

Mg–R	R	WBI	Natural Charge	Mg–R	R	WBI	Natural Charge
	C^{1}	0.3053	0.02274		C^{1}	0.2683	0.00976
	C^{12}	0.2953	0.03280		C^{12}	0.2670	0.02689
	C^{23}	0.2832	0.03193		C^{27}	0.3936	–1.30001
	Br^{1}	0.4846	–0.66520		O^{1}	0.1259	–0.69346
	Mg	–	1.12487		Mg	–	1.29442

7 $(^{Me}NHC)_2MgBr_2$ — **8a** $(^{Me}NHC)_3MgBr_2$

Mg–R	R	WBI	Natural Charge	Mg–R	R	WBI	Natural Charge
	C^{1}	0.2874	0.07899		C^{1}	0.2872	0.08595
	C^{8}	0.2874	0.07899		$C^{1'}$	0.2872	0.08595
	Br^{1}	0.4945	–0.68177		$C^{1''}$	0.2872	0.08595
	Br^{2}	0.4945	–0.68177		Br^{1}	0.3573	–0.73825
	Mg	–	1.07675		Br^{2}	0.3573	–0.73825
					Mg	–	1.02670

$8b^{+}$ $[(^{Me}NHC)_3MgBr]^{+}$

Mg–R	R	WBI	Natural Charge
	C^{8}	0.3231	0.04107
	$C^{8'}$	0.3176	0.04751
	$C^{8''}$	0.3209	0.03652
	Br^{3}	0.5371	–0.65253
	Mg	–	1.07605

Table S3. WBI and natural charges for simplistic model Mg–R (R= ^{NHC}C, Br, $(Br)_2$, Me, O, ^{THF}O) compounds

	WBI (Mg–R)	Natural charge (Mg)	Natural charge (R)
$Mg(^{Me}NHC)^{2+}$	0.3870	1.75189	–0.26126
$Mg(^{iPr}NHC)^{2+}$	0.3706	1.72138	–0.21918
$MgBr^+$	0.7178	1.59622	–0.59622
$MgBr_2$	0.6246	1.29674	–0.64836
$Mg(Me)^+$	0.7994	1.44614	–1.26468
MgO^+	0.5641	1.67888	–0.67888
MgO	1.5202	1.00594	–1.00594
$Mg(THF)^{2+}$	0.1624	1.90383	–0.90464

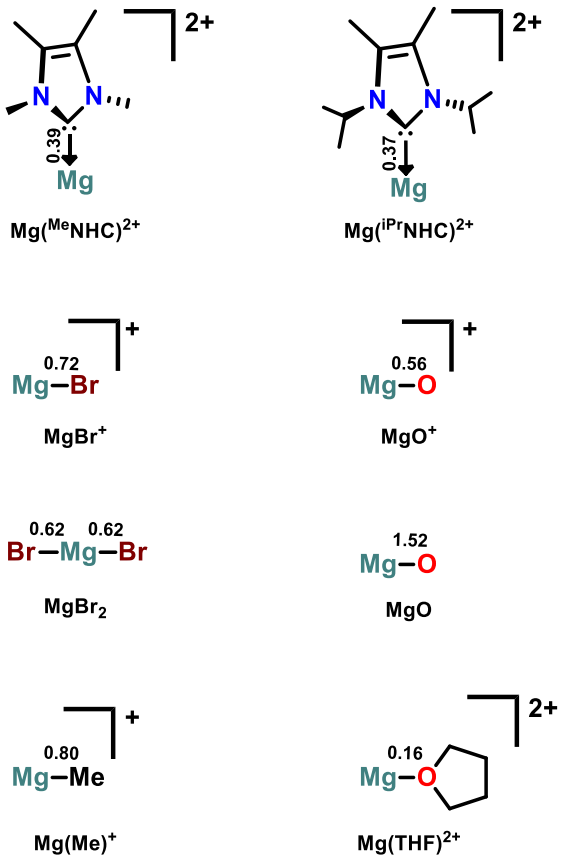

Figure S28: 2D representation of simplistic model Mg–R (R = ^{Me}NHC, ^{iPr}NHC, Br, $(Br)_2$, Me, O, THF) compounds with corresponding WBIs.

Molecular Orbitals for 2

MO 221 LUMO –2.92 eV (–0.10713 a.u.)

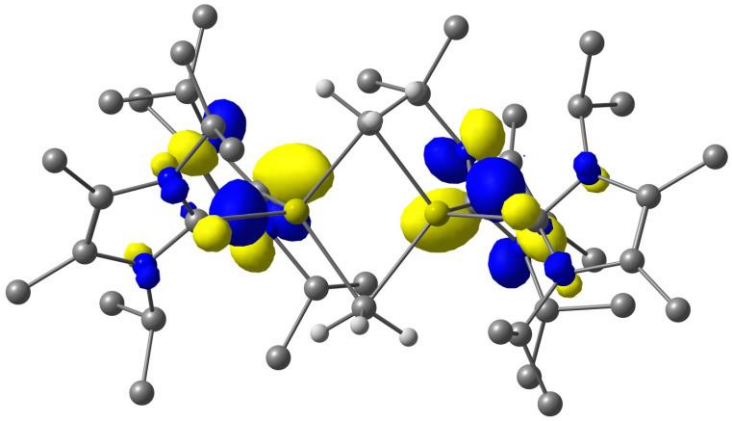

MO 220 HOMO –12.58 eV (–0.46225 a.u.)

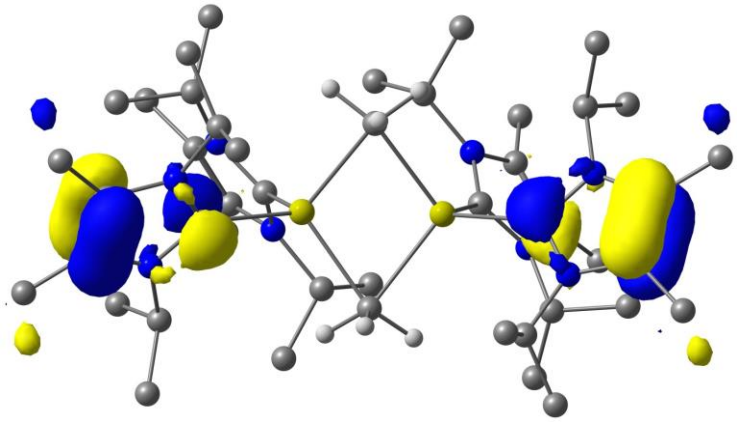

Figure S29. Frontier molecular orbitals (HOMO and LUMO) for **2**. Select hydrogen atoms not pictured for clarity.

MO 215 HOMO – 5 –14.13 eV (–0.51924 a.u.)

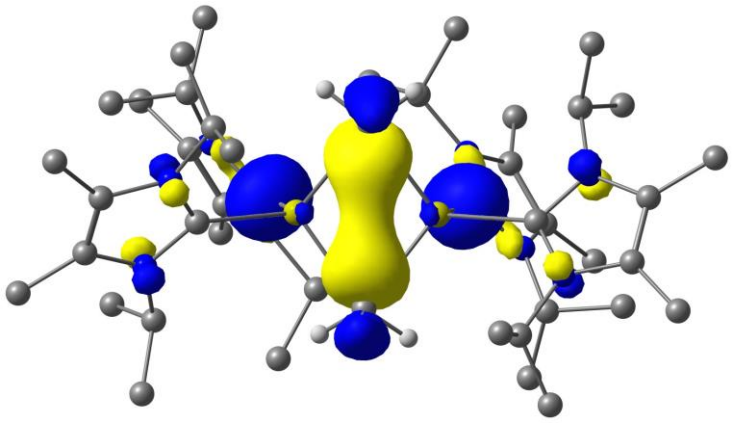

Figure S30. HOMO – 5 highlighting Mg(μ-Me) interaction in **2**. Select hydrogen atoms not pictured for clarity.

MO 216 HOMO – 4

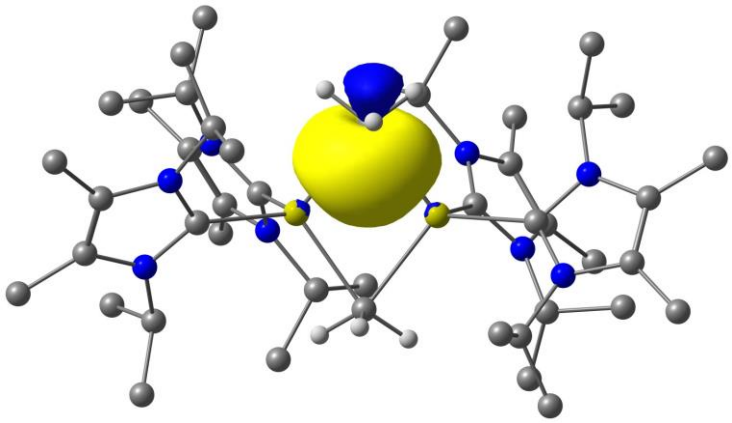

MO 215 HOMO – 5

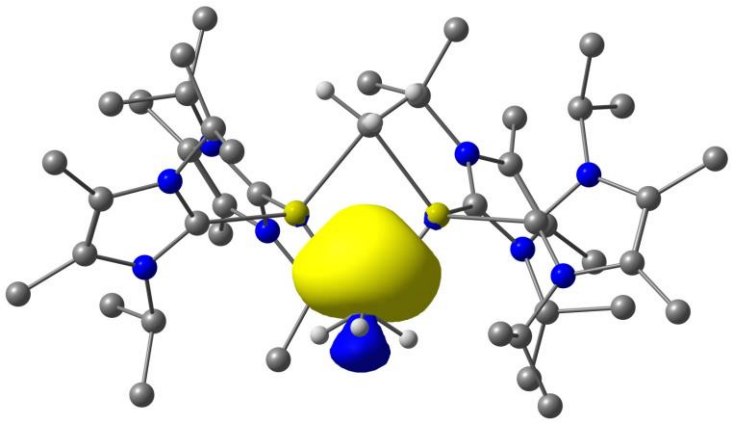

Figure S31. Pipek-Mezey Localized Molecular Orbitals for HOMO – 4 and HOMO – 5. Select hydrogen atoms not pictured for clarity.

References

1. Bruker *Saint; SADABS; APEX3*, Bruker AXS Inc.: Madison, Wisconsin, USA, 2012
2. Sheldrick, G. M., SHELXT– Integrated space-group and crystal-structure determination. *Acta Crystallogr., Sect. A: Found. Crystallogr.* **2015,** *71*, 3-8.
3. Dolomanov, O. V.; Bourhis, L. J.; Gildea, R. J.; Howard, J. A. K.; Puschmann, H., OLEX2: a c omplete structure solution, refinement and analysis program. *J. Appl. Crystallogr.* **2009,** *42*, 339-341.
4. Sheldrick, G. *CELL_NOW, version 2008/4*, Georg-August-Universitat Göttingen: Göttingen, Germany, 2008
5. Frisch, M. J.; Trucks, G. W.; Schlegel, H. B.; Scuseria, G. E.; Robb, M. A.; Cheeseman, J. R.; Scalmani, G.; Barone, V.; Petersson, G. A.; Nakatsuji, H.; Li, X.; Caricato, M.; Marenich, A. V.; Bloino, J.; Janesko, B. G.; Gomperts, R.; Mennucci, B.; Hratchian, H. P.; Ortiz, J. V.; Izmaylov, A. F.; Sonnenberg, J. L.; Williams; Ding, F.; Lipparini, F.; Egidi, F.; Goings, J.; Peng, B.; Petrone, A.; Henderson, T.; Ranasinghe, D.; Zakrzewski, V. G.; Gao, J.; Rega, N.; Zheng, G.; Liang, W.; Hada, M.; Ehara, M.; Toyota, K.; Fukuda, R.; Hasegawa, J.; Ishida, M.; Nakajima, T.; Honda, Y.; Kitao, O.; Nakai, H.; Vreven, T.; Throssell, K.; Montgomery Jr., J. A.; Peralta, J. E.; Ogliaro, F.; Bearpark, M. J.; Heyd, J. J.; Brothers, E. N.; Kudin, K. N.; Staroverov, V. N.; Keith, T. A.; Kobayashi, R.; Normand, J.; Raghavachari, K.; Rendell, A. P.; Burant, J. C.; Iyengar, S. S.; Tomasi, J.; Cossi, M.; Millam, J. M.; Klene, M.; Adamo, C.; Cammi, R.; Ochterski, J. W.; Martin, R. L.; Morokuma, K.; Farkas, O.; Foresman, J. B.; Fox, D. J. *Gaussian 16 Revision B.01*, Wallingford, CT, 2016
6. Chai, J.-D.; Head-Gordon, M., Long-range corrected hybrid density functionals with damped atom–atom dispersion corrections. *Phys. Chem. Chem. Phys.* **2008,** *10*, 6615-6620.
7. (a) Kendall, R. A.; Dunning, T. H.; Harrison, R. J., Electron affinities of the first-row atoms revisited. Systematic basis sets and wave functions. *J. Chem. Phys.* **1992,** *96*, 6796-6806; (b) Dunning Jr, T. H., Gaussian basis sets for use in correlated molecular calculations. I. The atoms boron through neon and hydrogen. *J. Chem. Phys.* **1989,** *90*, 1007-1023; (c) Peterson, K. A.; Shepler, B. C.; Figgen, D.; Stoll, H., On the Spectroscopic and Thermochemical Properties of ClO, BrO, IO, and Their Anions. *J. Phys. Chem. A* **2006,** *110*, 13877-13883; (d) Peterson, K. A., Systematically convergent basis sets with relativistic pseudopotentials. I. Correlation consistent basis sets for the post-d group 13–15 elements. *J. Chem. Phys.* **2003,** *119*, 11099-11112; (e) Peterson, K. A.; Figgen, D.; Goll, E.; Stoll, H.; Dolg, M., Systematically convergent basis sets with relativistic pseudopotentials. II. Small-core pseudopotentials and correlation consistent basis sets for the post-d group 16–18 elements. *J. Chem. Phys.* **2003,** *119*, 11113-11123.
8. Frisch, M. J.; Trucks, G. W.; Schlegel, H. B.; Scuseria, G. E.; Robb, M. A.; Cheeseman, J. R.; Scalmani, G.; Barone, V.; Petersson, G. A.; Nakatsuji, H.; Li, X.; Caricato, M.; Marenich, A. V.; Bloino, J.; Janesko, B. G.; Gomperts, R.; Mennucci, B.; Hratchian, H. P.; Ortiz, J. V.; Izmaylov, A. F.; Sonnenberg, J. L.; Williams; Ding, F.; Lipparini, F.; Egidi, F.; Goings, J.; Peng, B.; Petrone, A.; Henderson, T.; Ranasinghe, D.; Zakrzewski, V. G.; Gao, J.; Rega, N.; Zheng, G.; Liang, W.; Hada, M.; Ehara, M.; Toyota, K.; Fukuda, R.; Hasegawa, J.; Ishida, M.; Nakajima, T.; Honda, Y.; Kitao, O.; Nakai, H.; Vreven, T.; Throssell, K.; Montgomery Jr., J. A.; Peralta, J. E.; Ogliaro, F.; Bearpark, M. J.; Heyd, J. J.; Brothers, E. N.; Kudin, K. N.; Staroverov, V. N.; Keith, T. A.; Kobayashi, R.; Normand, J.; Raghavachari, K.; Rendell, A. P.; Burant, J. C.; Iyengar, S. S.; Tomasi, J.; Cossi, M.; Millam, J. M.; Klene, M.; Adamo, C.; Cammi, R.; Ochterski, J. W.; Martin, R. L.; Morokuma, K.; Farkas, O.; Foresman, J. B.; Fox, D. J. *Gaussian 09 Revision D. 01*, Wallingford, CT, 2016
9. Lu, T.; Chen, F., Multiwfn: A multifunctional wavefunction analyzer. *J. Comput. Chem.* **2012,** *33*, 580-592.
10. Pipek, J.; Mezey, P. G., A fast intrinsic localization procedure applicable for ab initio and semiempirical linear combination of atomic orbital wave functions. *J. Chem. Phys.* **1989,** *90*, 4916-4926.
11. Zhurko, G. A. Chemcraft. Ivanonvo, Russia 2005.

.